Desalination and Water Treatment
www.deswater.com

doi: 10.5004/dwt.2019.24149

157 (2019) 18–28
July

Negatively charged polyamide thin film composite membrane with ultra-smooth selective layer and excellent organic solvent resistance for nanofiltration application

Shanshan Yang[a], Ya'nan Xing[a], Jinmiao Zhang[a], Baowei Su[a,*], Bishnupada Mandal[b,*], Xueli Gao[a,*], Congjie Gao[a]

[a]*Key Laboratory of Marine Chemistry Theory and Technology (Ocean University of China), Ministry of Education; College of Chemistry & Chemical Engineering, Ocean University of China, Qingdao 266100, China, Tel./Fax: +86−532−66786371; email: subaowei@ouc.edu.cn (B. Su)*

[b]*Department of Chemical Engineering, Indian Institute of Technology Guwahati, Guwahati 781039, India, Tel. +91 361 2582256/+91-9957181980; Fax: +91 361 2582291; email: bpmandal@iitg.ac.in*

Received 30 May 2018; Accepted 17 March 2019

ABSTRACT

This work reports a novel negatively charged thin film composite–polyamide (TFC-PA) membrane with ultra-smooth selective layer prepared via interfacial polymerization for nanofiltration (NF) and organic solvent nanofiltration applications. Alkali-modified polyacrylonitrile (PAN) ultrafiltration (UF) was used as substrate. Poly(ethyleneimine) (PEI) and trimesoyl chloride were used as functional monomers of aqueous and organic solution, respectively. The effect of supporting salt concentration in the aqueous PEI solution on the improvement of the PEI assembly regularity was investigated. Under optimal conditions, the average surface roughness (Sa) of the prepared TFC-PA membrane surface was 5.4 nm. It achieved a salt rejection of 97.6% and a flux of 38.2 L m^{-2} h^{-1} for 2,000 mg L^{-1} Na_2SO_4 aqueous solution at 1.0 MPa and 20°C. Furthermore, it maintained nearly constant rejection and flux after being immersed in methanol, *n*-hexane, acetone and ethyl acetate, respectively, for 60 d, indicating the excellent resistance to these solvents.

Keywords: Nanofiltration; Interfacial polymerization (IP); Ultra-smooth; Supporting salt; Solvent resistance

1. Introduction

Nanofiltration (NF) membranes usually have high rejection of multivalent ions and low rejection of monovalent ions, and with a molecular weight cut-off (MWCO) of 200–1,000 Da, which make it suitable for the separation of multivalent ions from monovalent ions, as well as organic matters with molecular weight greater than 200 Da from aqueous or organic solutions. Although the NF membrane separation technology has been applied in many industrial processes, the further application of NF as an efficient separation technology on different industries requires plenty of membranes with higher quality due to the complex compositions of solutions. Nowadays, several typical membranes such as integrally skinned membranes [1], dual-layer membranes [2,3] and thin film composite membranes have been developed for NF and organic solvent nanofiltration (OSN).

Thin film composite polyamide [3] (TFC-PA) membranes fabricated by interfacial polymerization (IP) on porous ultrafiltration (UF) support have already attracted a lot of attentions [4–6], since TFC-PA membranes have the potential to achieve higher permeance than the integrally skinned membranes [6]. Thinner thickness, larger

* Corresponding authors.

porosity and smaller mean pore diameter are expected for the selective layer to enhance the permeance and rejection of NF membranes, since the selective layer dominates the separation performance as well as the antifouling and oxidative resistance of TFC membranes [7,8]. In order to achieve ultrafast permeance and high rejection, the IP process should be controlled perfectly. Recently, Santanu Karan and Livingston [4] reported a new method to fabricate sub-10 nm PI NF membrane with ultrafast solvent transport, in which the sacrificial layer of cadmium hydroxide nanostrands has been formed as an interlayer on an UF support membrane before the IP process and removed after the IP process to control the IP conditions perfectly. The rejection for methyl organic (MW = 327.3 g mol) and the flux for methanol of the sub-10 nm membrane have been reported as 98.9% and 52 L $m^{-2} h^{-1} bar^{-1}$, respectively. Zhang et al. [8] prepared a TFC NF membrane via IP with polyphenol coating as an interlayer to control the diffusion of monomer in the aqueous phase solution. In this case, the flux increased triple folds to 10.5 L $m^{-2} h^{-1} bar^{-1}$ with above 98% rejection for Na_2SO_4.

Recently, multi-amine such as polyethyleneimine (PEI) has been used as aqueous monomer for the IP reaction. PEI is a kind of water-soluble polyamine polymer. It is relatively easier to control the IP process using PEI as aqueous monomer compared with those using small molecular amines as aqueous monomer, since the transfer of PEI from aqueous solution to organic solution was slow [9]. As a kind of cationic polyelectrolyte in aqueous solution, PEI has gained many applications in LBL membrane preparation [10–12]. Several researchers have investigated the preparation of PA-TFC membranes by using IP reaction of PEI and trimesoyl chloride (TMC). Wu et al. [12] prepared a kind of positively charged multiple polyamide NF membranes via IP using 3.5 wt.% PEI and 0.7 wt.% TMC and the resultant membrane maintained a Na_2SO_4 rejection of 80.5% and a pure water flux of 24.5 L $m^{-2} h^{-1}$ at 0.8 MPa. Fang et al. [9] successfully prepared IP hollow fiber NF membranes using PEI and TMC on PES substrate. The reported NF membrane achieved an inorganic salt rejection rate of 80.6% for 1,000 mg L^{-1} $MgSO_4$ aqueous solution, and a high flux of about 20 L $m^{-2} h^{-1}$ at 0.2 MPa, proving excellent prospect for softening of low concentration brackish water.

Generally, the adsorption of aqueous monomer at low concentration on substrate surface is not adequate, or the arrangement of the aqueous monomer might be very loose. Therefore, the reactive monomers or polymers with higher concentrations have been used in the aqueous monomer solutions, as well as in the organic solutions. For instance, PEI concentration used in this situation was usually about 3–5 wt.% [12–15].

Until now, most of the PA-TFC membranes fabricated with PEI and TMC are aiming at the applications in aqueous solutions. Recently, a few research works were carried out on the applications of PA-TFC NF membrane for the separation of organic solvent solutions [15,16]. However, relatively few works were carried out on the preparation of PEI-based TFC membrane with good solvent resistance. PEI has been reported as a generic material for composite NF membrane, and the structural stability of PEI-based membranes can be facilely enhanced by cross-linking [14,15,17,18]. Recently, positively charged nanofiltration membranes using PEI via cross-linking were fabricated by Wang et al. [19], which showed a rejection of 95% for methylene blue (MW = 319.86 g mol^{-1}) and a relatively high antifouling properties for different organic dyes.

This work demonstrates our efforts to fabricate a dense, thin and defect-free TFC membrane with high flux and high rejection by a simple method. We investigated systematically the preparation conditions of a novel TFC-PA membrane via IP using PEI and TMC for NF application. Very low concentrations of PEI and TMC were selected for the IP process. We reasonably envision that the addition of NaCl to the aqueous PEI solution will improve the assembly regularity of PEI molecules on the substrate surface. Hence, NaCl as a kind of supporting electrolyte was added to the aqueous PEI solution to perfectly control the IP process. The chemical composition and morphology of the prepared membranes were investigated by Fourier transform infrared (FTIR), scanning electron microscopy (SEM) and atomic force microscope (AFM). Further, the separation performance, hydrophilicity and zeta potential were also examined. The solvent resistance of the prepared TFC membranes under the optimal preparation conditions was studied by immersing them in methanol, *n*-hexane, acetone, and ethyl acetate, respectively, for 60 d.

2. Experimental

2.1. Materials

Poly(ethyleneimine) (PEI) with a weight-average molecular weight of ~750,000 Da and a concentration of 50 wt.% PEI in water was purchased from Sigma-Aldrich (Shanghai, China) and was used without any further purification. TMC was procured from Alfa Aesar (Shanghai, China). Polyacrylonitrile (PAN) UF membrane with molecular weight cut-off (MWCO) of 50,000 Da was kindly supplied by Shanghai Mega Vision Membrane Engineering & Technology Co., Ltd. (Shanghai, China), and was hydrolyzed before use. NaOH, HCl, NaCl, KCl, $MgSO_4$, Na_2SO_4, methanol, *n*-hexane, acetone and ethyl acetate were analytical grade reagents provided by Shanghai Chemical Reagent Co. Ltd. (Shanghai, China), and were used as received without any further purification.

2.2. Preparation procedure

2.2.1. Pretreatment of UF substrate

The PAN UF membrane was first immersed in 2.0 M NaOH solution at 65°C for 1 h to perform caustic hydrolysis modification. Afterward, it was taken out, rinsed with deionized (DI) water to wash away the remaining caustic solution on the surface until the pH of the water after immersion became neutral. Then it was immersed in DI water for the further usage. The hydrolyzed PAN membrane was denoted as H-PAN.

2.2.2. Composite membrane preparation

PEI (0.2–0.8 wt.%) and NaCl (0–1.0 wt.%) were dissolved in DI water to prepare the aqueous monomer solution. TMC (0.1–0.4 wt.%) was dissolved in *n*-hexane to prepare the organic monomer solution. Usually, the NaCl concentration in the aqueous monomer solution was maintained at 0.50 M,

unless the effect of the supporting electrolyte concentration was investigated.

During the preparation of the TFC NF membrane, first, a piece of H-PAN substrate sheet was soaked in the aqueous monomer solution for 10–30 min to achieve sufficient adsorption of the amine monomer onto the substrate surface. Then the substrate sheet was taken out and the excess amine solution remaining on the membrane surface was drained off. The substrate was dried in the air for about 1 min until no droplets could be seen on its surface. Then it was dipped into the organic monomer solution for 30–250 s to conduct IP reaction and form a composite skin layer. Finally, it was taken out and dried in the air, and followed by a further post heat treatment at 70°C for 15 min. Thus a piece of virgin PA-TFC membrane (denoted as V-PA) was completed. The V-PA membrane was preserved in DI water to perform complete hydrolysis of the remaining acyl chloride group on the membrane surface. Thus, the PA-TFC membrane was finished successfully. The prepared PA-TFC membranes were reserved in the DI water before the separation performance test. The steps of the TFC membrane preparation process can be summarized in Table 1.

Without specification, the preparation conditions for the TFC membranes involved 0.40% PEI in 0.50 M NaCl aqueous solution, 0.20% TMC organic solution and 60 s reaction time.

2.3. Membrane characterization

Except for surface charge measurement, membrane samples were first dried in a vacuum oven at 45°C over 24 h before characterization.

2.3.1. ATR-FTIR measurements

Attenuated total reflectance Fourier transform infrared (ATR-FTIR) spectroscopy was used to investigate the chemical composition of the membrane surface before and after the IP reaction. The spectra with wave number ranging from 4,000 to 600 cm^{-1} was collected at a resolution of 2 cm^{-1} using a Nicolet magna-560 FTIR spectrophotometer.

2.3.2. Scanning electron microscopy

The surface and cross-section morphologies of the substrate as well as the TFC-PA OSN membranes were characterized using scanning electron microscopy (SEM, Hitachi S-4800, Japan). Membrane samples were sputter-coated with 5 nm thickness of gold on the membrane surface in advance. A magnification ratio of 100,000 and an accelerating voltage of 7.0 kV were used for the observation of the membrane surface. For the cross-section observation, the magnification ratio was set as 50,000.

2.3.3. Atomic force microscope

An AFM (Agilent 5400, Agilent Technologies, USA) was used to image the surface roughness of the membranes. Membrane morphology was measured directly in a scan size of 20 μm × 20 μm with a scan rate of 1.00 Hz at 256 × 256 resolution in tapping mode. The membrane surface roughness was measured based on scans of at least three different areas, and was calculated in terms of the average surface roughness (Sa).

2.3.4. Membrane surface hydrophilicity

The hydrophilicity of the substrate surface, the hydrolyzed substrate surface before and after PEI deposition, as well as the TFC-PA membrane after the IP reaction and the PA membrane after immersion in water was investigated by measuring contact angle of the surface using a Contact Angle Goniometer (DSA100, Kruss, Germany) with static sessile drop method. For each measurement, five drops of DI water (each drop was 1.0 μL) were dipped onto the surface of each sample and the contact angle was measured for each drop. An average value was obtained for each sample.

2.3.5. Membrane surface zeta potential

The surface charge of the composite membrane prepared by IP was measured using a self-made streaming potential apparatus with a symmetric clamping cell and Ag/AgCl electrodes. The apparatus and the measurement procedure was the same as presented elsewhere [20].

2.4. Evaluation of membrane performances

The performance of the fabricated membranes was evaluated considering their water permeability and salt rejection using single salt solution of 2,000 mg L^{-1} Na_2SO_4, NaCl, $MgCl_2$, $MgSO_4$, respectively. NF experiments were carried out using a cross-flow pressure filtration apparatus described in our former research work [21]. Each membrane sample was housed in a stainless steel cell with an active membrane area of 28.26 cm^2.

All tests were performed at 1.0 MPa and room temperature (20°C) with single electrolyte solution. The observed

Table 1
Steps of the TFC membranes preparation process

Step	Membranes	Detail description
1	H-PAN	PAN membrane after hydrolyzed in 2.0 M NaOH solution at 65°C for 1 h and then rinsed with DI water
2	H-PAN/PEI	H-PAN membrane after soaked in the aqueous PEI solution for 10–30 min
3	V-PA/TFC	H-PAN/PEI membrane after dipped into the organic monomer solution for 30–250 s and a further post-heat treatment at 70°C for 15 min
4	PA/TFC	V-PA TFC membrane after reservation in DI water

rejection (R) of the NF membranes for single salt solution and the flux (J_v) were calculated as described elsewhere [20]. Duplicates were performed for each procedure. The average values of the salt rejections for each procedure were used for discussion.

2.5. Solvent resistance

To investigate the effect of IP reaction on the solvent resistance of the prepared TFC membranes, the prepared PA membranes were soaked in methanol, acetone, *n*-hexane, ethyl acetate, respectively, for 0–60 d. Afterward, they were taken out from the organic solvent, washed and soaked in DI water for 2 h to remove the residual organic solvent. Then the separation performance was measured. Shortly thereafter, the membranes were continually soaked back into the previous solvent.

3. Results and discussion

3.1. Mechanism of the membrane preparation process

3.1.1. ATR-FTIR analysis

The ATR-FTIR spectra of the surface of the H-PAN substrate and the prepared PA composite membranes are shown in Fig. 1.

For the H-PAN substrate, the absorption peak at 2,243 cm^{-1} belongs to the bending vibration of the unhydrolyzed nitrile groups (–C°N) on the PAN chains [22]. However, the peak of the nitrile groups decreased gradually during the preparation process, implying that the H-PAN substrate surface was gradually covered by the depositing PEI molecules and the subsequent skin layer formed by the IP reaction. The absorption peaks at 3,433 and 1,731 cm^{-1} correspond to the characteristic peaks of O–H and C=O bonds [23], respectively, which demonstrated that certain amount of nitrile groups on the PAN substrate surface, were hydrolyzed and converted to carboxylic groups.

In the spectrum of the H-PAN/PEI membrane, the emerging absorption peak at 1,572 cm^{-1} corresponds to the in-plane bending vibration of N–H bond of PEI molecules [16], which demonstrated the deposition of PEI molecules on the H-PAN substrate surface.

In the spectrum of the PA composite membrane, the peak at 2,243 cm^{-1} belongs to the characteristic peak of the nitrile groups of the H-PAN substrate, since the detection depth of ATR-FTIR technique was micron grade. The absorption peak at 2,243 cm^{-1} became weaker during the preparation process, indicating that the substrate surface was gradually covered by the IP reaction layer. New absorption peaks which emerged at 1,639 and 1,552 cm^{-1} were assigned to the C=O stretching vibrations (amide I) and N–H in-plane bending (amide II) [24], respectively, proved the existence of amide (–CONH–) functionalities formed by the amidation reaction between $–NH_2$ groups of PEI chain and –COCl groups of TMC.

3.1.2. Contact angle analysis

The contact angles of the surface of the PAN substrate, the H-PAN substrate, the PAN/PEI layer, the virgin PA (V-PA) and the PA membranes are shown in Fig. 2.

It can be seen from Fig. 2 that the contact angles of the membrane surfaces showed a decreasing trend along the preparation process (except the V-PA) and the hydrophilicity increased. The contact angle of the PAN substrate surface decreased from 35° to 33° owing to the alkali modification of the –CN groups of the PAN substrate to –COOH groups. The deposition of PEI layer caused further decrease of the contact angle down to 28°, suggesting the strong hydrophilic nature of PEI polyelectrolyte due to hydrophilic $–NH_2$ groups. After the IP reaction, the contact angle of the virgin PA membrane increased slightly up to 32°, since the formed amide groups were slightly less hydrophilic than PEI molecules [25].

The further hydrolysis of the virgin PA membrane after immersion in pure water increased hydrophilicity apparently,

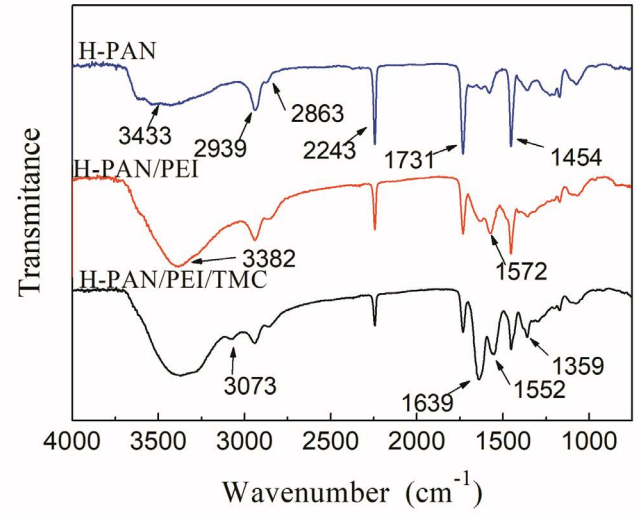

Fig. 1. FTIR spectra of the surface of the H-PAN substrate and H-PAN/PEI and H-PAN/PEI/TMC composite membranes.

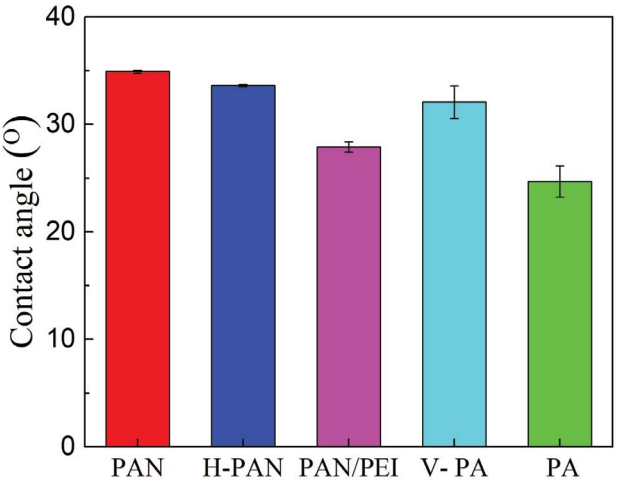

Fig. 2. Contact angles of the surface of the PAN substrate, the H-PAN substrate, the PAN/PEI layer, the virgin PA (V-PA) and the PA membrane.

the contact angle dropped to 24°, suggesting the hydrolysis of the remaining unreacted acyl chloride (–COCl) groups on the V-PA membrane surface to carboxylic acid when the V-PA membrane was immersed in pure water [5]. This is superior to the contact angle of the well-known and wildly used commercial DOW NF270 membrane, which is reported to be around 27° [26], demonstrating the excellent hydrophilicity of the PA membrane prepared in this work.

3.2. Factors affecting the performance of the PA membrane

3.2.1. PEI concentration

Effect of PEI concentration on the separation performance of the PA membrane is depicted in Fig. 3.

It was observed from Fig. 3 that when the aqueous PEI concentration was lower than 0.40%, Na_2SO_4 rejection showed a sharp increase in the trend with the increase of PEI concentration, while the flux showed a reverse trend. The sharp increase of salt rejection and the rapid decline of the flux implied that at this PEI concentration range, more PEI molecules deposited on the substrate membrane surface, thus the subsequent - PA function layer became denser and thicker gradually. With the further increase of the aqueous PEI concentration up to 0.80%, Na_2SO_4 rejection decreased marginally and the flux increased gradually. This is presumably due to the deficit of the TMC molecules that lead to a relatively lower cross-linking density on the V-PA membrane, resulting in higher flux and lower rejection at higher PEI concentration.

It can also be seen from Fig. 3 that when the PEI concentration was kept at about 0.40%, the TFC-PA membranes achieved an optimal separation performance, with the Na_2SO_4 rejection reaching a maximum value of 97% and the permeation flux reaching about 40 L m^{-2} h^{-1} at 1.0 MPa. It should be noted that this PEI concentration is quite low compared with those of other research works [12–15] which is usually about 3%–5% without any supporting electrolyte used, indicating that with the addition of the supporting electrolyte, an excellent separation performance could be achieved at lower aqueous PEI concentration.

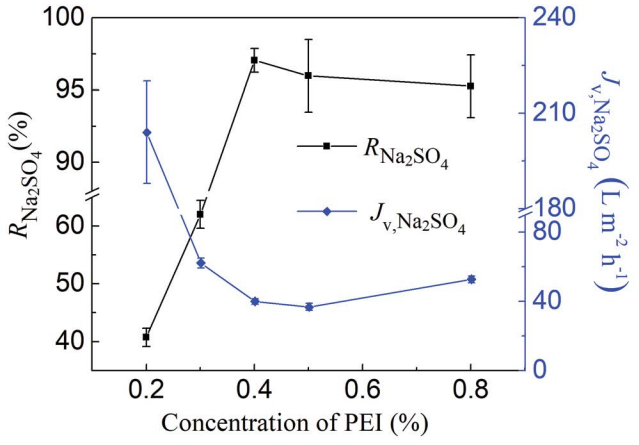

Fig. 3. Effect of PEI concentration on the separation performance of the PA membrane.

3.2.2. TMC concentration

The effect of TMC concentration on the separation performance of the PA composite membranes is shown in Fig. 4. When the TMC is less than 0.4%, the rejection increased marginally whereas the flux maintained essentially constant. As the separation performance of the composite NF membranes was good at the TMC concentration range between 0.15% and 0.30%, the TMC concentration of 0.20% was selected for further investigation.

3.2.3. Supporting electrolyte concentration

The effect of the concentration of the aqueous supporting electrolyte on the performance of the prepared PA-TFC membranes is shown in Fig. 5. As can be seen, the rejection for Na_2SO_4 was less than 85% when no supporting electrolyte was added to the aqueous PEI solution. However, when the concentration of NaCl in the aqueous solution was higher than 0.50 M, the rejection of the prepared membrane could be as high as 95%, which demonstrated that NaCl as a kind of supporting electrolyte in the aqueous PEI solution could

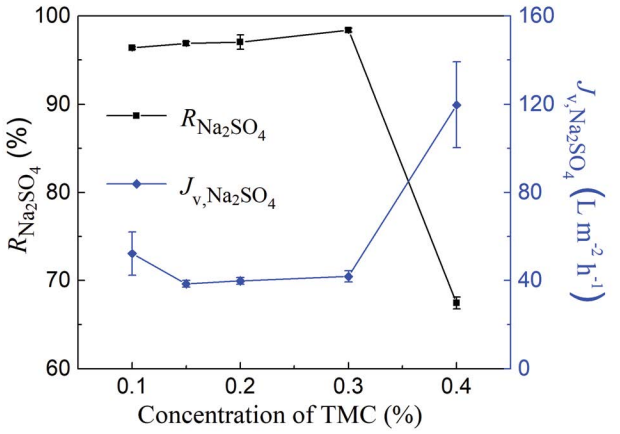

Fig. 4. Effect of TMC concentration on the separation performance of PA membrane.

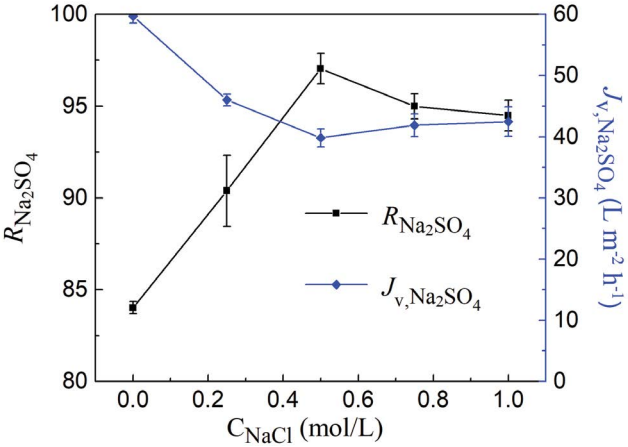

Fig. 5. Effect of salt concentration on the separation performance of the PA membrane.

improve the separation performance of the IP composite NF membrane at much lower PEI concentration.

It was reported that the presence of salt in polyelectrolyte solutions drastically affects the polyelectrolyte chain configuration in the bulk solution [27,28], induces the folding of the polyelectrolyte chain from fully extended, rod-like configuration to random coil configuration when it adsorbs onto the substrate surface [27], and increases the multilayer thickness [28]. Therefore, the deposition amount and the deposition density of the PEI molecules on the substrate surface as well as the effective thickness of the PEI layer increased with the concentration of NaCl. This improved the IP reaction and the separation performance of the prepared PA composite membranes, and resulted in a slight increase of the rejection and a slight decrease of the flux. Nevertheless, when the NaCl concentration increased higher than 0.50 M, the further increase of the NaCl concentration caused the stronger coil of the PEI molecules which cannot be well packed [29], thus defects are enlarged, resulting in a slight decrease of rejection and a slight increase of flux.

As the Na_2SO_4 rejection has a maximum value when the NaCl concentration was 0.50 M, in the following membrane preparation experiments, the NaCl concentration was selected as 0.50 M.

3.2.4. Immersion time in aqueous PEI solution

The effect of the deposition time of the aqueous PEI solution on the separation performance of the formed PA-TFC membrane is shown in Table 2. With the prolonging deposition time of the aqueous solution, the flux of the formed PA-TFC membranes for both Na_2SO_4 and NaCl solutions increased, and the salt rejection decreased accordingly.

Theoretically, self-assembly of macromolecules forms a single layer of molecules (<10 nm) on substrate [27]. However, as the highly branch characteristic of the PEI macromolecule, the actual deposition was not ideal and showed some extent of irregularity, and there may be a plurality of deposition layers. Therefore, the number of the depositing molecules and the thickness of the depositing layer increased with the increase of the immersion time. However, as all the deposited PEI molecules have the same type of charge, they were mutually exclusive with each other, resulting in a looser depositing layer with the increasing amount of the deposited molecules. This in turn resulted in the decrease of the rejection and the increase of the flux, which confirmed that there should be an optimal deposition time in the LBL self-assembly membrane preparation process [21,30–32]. In our work, we chose 10 min as the optimal aqueous immersion time.

Table 2
Effect of the immersion time of aqueous PEI solution on the separation performance of the PA-TFC membrane

	Na_2SO_4 solution		NaCl solution	
t_{PEI} (min)	R (%)	J_V (L m^{-2} h^{-1})	R (%)	J_V (L m^{-2} h^{-1})
10	97.6	38.25	66.6	38.73
20	91.8	48.86	61.4	54.10
30	89.9	62.33	57.4	62.38

3.2.5. IP reaction time

The effect of the IP reaction time on the separation performance of the TFC-PA membrane is shown in Fig. 6. As depicted in this figure, when the IP reaction time was set at 30 s, the flux and the rejection of the PA membranes for Na_2SO_4 solution were already about 30 L m^{-2} h^{-1} and 98.0%, respectively, demonstrating that the substrate membrane surface was covered with an active layer successfully. With the IP reaction time increased from 30 to 90 s, the flux increased significantly, accompanied by a marginal decrease of rejection. This is different from the ordinary IP reaction of m-phenylenediamine (MPD) and TMC because of the highly branched characteristic nature of the PEI macromolecule. PEI would be more easily hindered during the diffusion process due to the formation of the dense selective layer, suggesting there would be more unreacted acyl chloride groups, which improved greatly the membrane surface hydrophilicity after the post hydrolysis and increased the flux of the membrane. Since the rejection maintained very high at 60 s, we chose 60 s as an optimal IP reaction time in the following experiments.

3.3. Separation performance of the prepared PA membrane

The separation performance of the prepared TFC NF membrane is shown in Fig. 7. As observed from Fig. 7, the rejection sequence of the prepared TFC NF membrane under optimal preparation conditions for the four kinds of inorganic salts was $R_{Na_2SO_4} > R_{MgSO_4} > R_{MgCl_2} > R_{NaCl}$. The rejection of Na_2SO_4 is higher than that of NaCl, and the rejection of $MgSO_4$ is higher than that of $MgCl_2$, demonstrating the typical characteristic of negatively charged membranes [33,34]. It is usually considered that the separation performance of NF membranes is a mutual effect of the steric hindrance and an electrostatic repulsion mechanism [35]. For negatively charged NF membranes with electrostatic repulsion as the dominant mechanism, rejection of multivalent cations should be lower than that of monovalent cations according to the Donnan exclusion. However, the NF membranes prepared in this experiment had a much higher rejection for $MgCl_2$ than that for NaCl, which indicated that steric

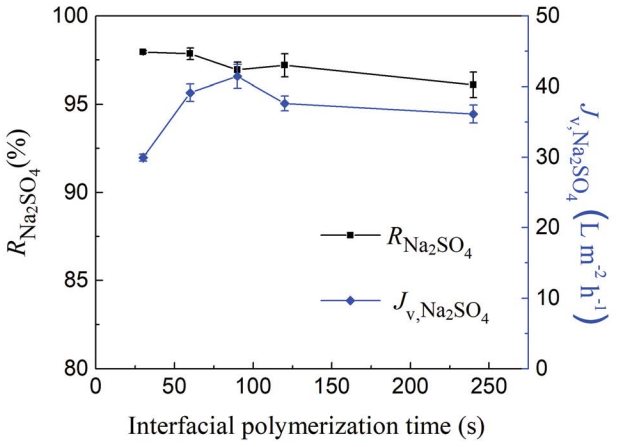

Fig. 6. Effect of IP reaction time on the separation performance of the PA-TFC membrane.

hindrance was also an important retention mechanism for the prepared NF membrane in addition to the electrostatic repulsion effect.

The comparison of the separation performance of the TFC NF membrane fabricated in this work with those of others prepared using PEI in literatures as well as the commercial NF90 (DOW-Filmtec, USA) membrane is shown in Table 3. It can be seen that the prepared NF membrane in this work has much higher selective rejections for divalent ions than monovalent ions compared with other TFC NF membranes prepared using PEI. The flux of the prepared NF membrane in this work is also quite high as compared with those of other TFC NF membranes which have about the same high rejection of divalent ions. The prepared PA-TFC membrane has a relative looser surface compared with the commercial NF90 membrane, which was indicated by the relative higher flux and relative lower rejection for NaCl and $MgSO_4$ than that of the latter membrane.

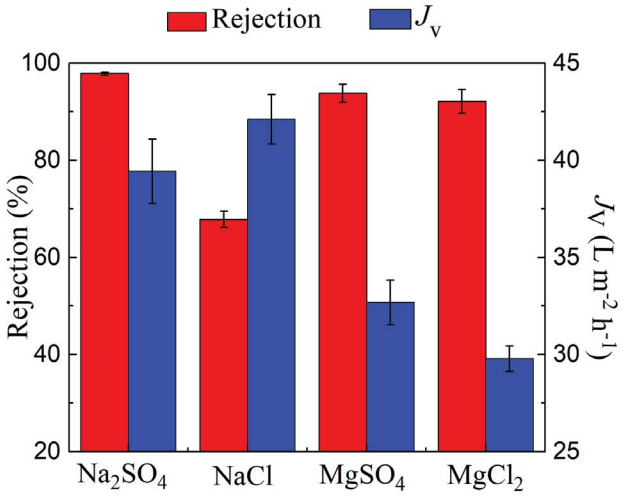

Fig. 7. Separation performance of the prepared PA composite membrane for different inorganic salt solution.

3.4. Morphology of the prepared membranes

SEM images of the H-PAN substrate and the prepared PA-TFC membranes are shown in Fig. 8. Many intensive pores on the H-PAN substrate surface were observed from Fig. 8a$_1$. However, the number of the pores decreased and the original large pores changed into fine thread-like pores after the IP between PEI and TMC, which is similar to the results reported by Zhao and Wang [41].

The deposition of the PEI molecules on the substrate is somewhat like the "layer by layer" assembly. As we know that the thickness of one bilayer is usually below 10 nm [27], the thickness of the IP skin layer we prepared should, therefore, be very thin. The cross-sectional SEM images proved that there is essentially no difference between the thickness of the H-PAN substrate (Fig. 8a$_2$) and that of the PA-TFC membrane (Fig. 8b$_2$).

It can be seen from Fig. 9 that the H-PAN substrate surface was relatively smooth (Fig. 8a), with an average surface roughness (Sa) of about 6.0 nm. After the formation of the PA-TFC layer on the substrate, the Sa of the surface was 5.4 nm. There were almost no defects on the surface of the prepared TFC-PA NF membranes. This was presumably due to the evenly distributed amine groups of the hyper branched PEI polymer, which served as uniform reactive sites after the PEI macromolecules were deposited onto the H-PAN substrate surface [12].

3.5. Membrane surface charge

As can be seen from Fig. 10, the isoelectric point of the H-PAN substrate was below 4.0. This was mainly attributed to the effect of the alkali modification that hydrolyzes the –CN groups on the PAN substrate surface to carboxyl groups (COOH), and further to carboxylate groups (COO^-).

Table 3
Comparison of the separation performance of NF membrane prepared in this work with those of the state-of-the-art composite NF membrane prepared using PEI as well as the commercial Dow-Filmtec NF90 membrane

Membranes	J_V* (L m^{-2} h^{-1})	Solute rejection (%)				C_{salt} (g L^{-1})	P (MPa)	Reference
		Na_2SO_4	NaCl	$MgCl_2$	$MgSO_4$			
PAN/PEI + NaCl/TMC flat sheet[a+]	43	97.6	66.6	92.1	93.7	2	1.0	This work
PES/PEI/TMC hollow fiber[b]	21.8	54.2	41.2	96.7	80.6	1	0.2	[9]
PEI/TMC flat sheet[c]	24.5	80.5	85.1	95.1	94.4	0.5	0.8	[12]
PEI/EHT/GO/TMC flat sheet[c]	26	13.4	~42	92.8	~22	1	0.8	[36]
PEI/PDA-MWCNTs/TMC flat sheet[b]	83.5	45.2	33.8	91.5	76.1	1	0.6	[37]
P84/PEI/GA hollow fiber[c]	8.7	>90	90	>90	>90	1	0.5	[38]
Dow-Filmtec NF90[c]	32.2	–	90	–	97	2	0.48	[39]
PEI/HACC/TiO_2/TMC flat sheet[d]	6.8	26.9	10.7	34.6	32.4	1	0.4	[13]
PEI-Dex + PEI/TMC flat sheet[c]	43	84	37	85	–	1.5	0.5	[40]
PEI-g-SBMA/TMC flat sheet[c]	26.4	50.4	7.1	47	~50	1	0.2	[24]

[+] Preparation conditions: 0.4 % PEI (0.5 M NaCl), 0.2 % TMC, t_{IP} = 60 s; heat treatment at 70°C for 15 min.
* Permeation flux, [a] NaCl; [b] $MgCl_2$; [c] pure water; [d] Na_2SO_4 feed solution.

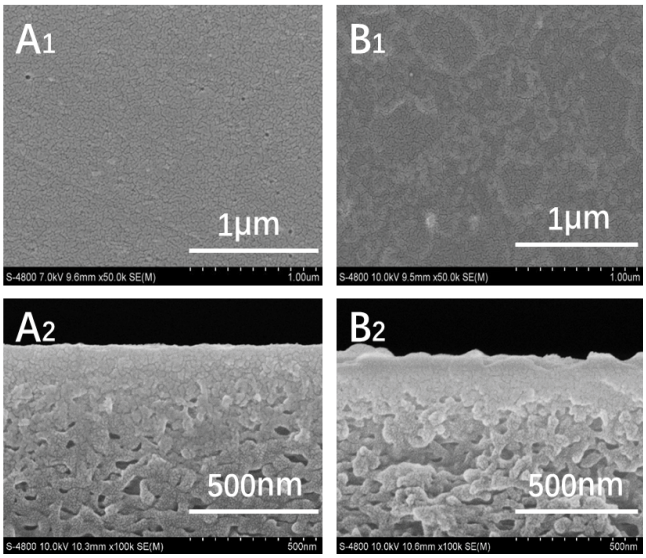

Fig. 8. SEM images of the membrane surface and cross-sectional morphology. (a) H-PAN substrate and (b) PA-TFC membrane.

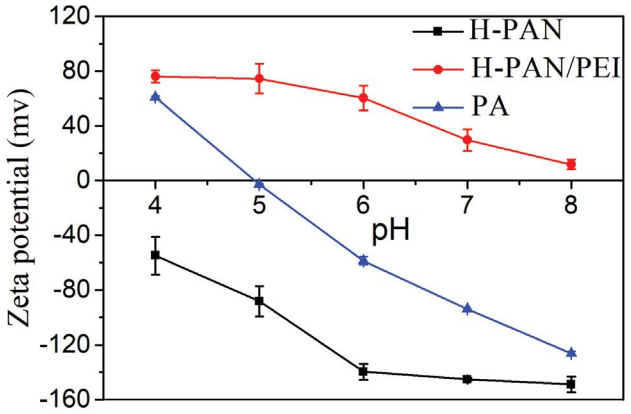

Fig. 10. Variation of zeta potential of the H-PAN, H-PAN/PEI, and the TFC-PA membrane with pH (Test conditions: 0.001 M KCl, room temperature).

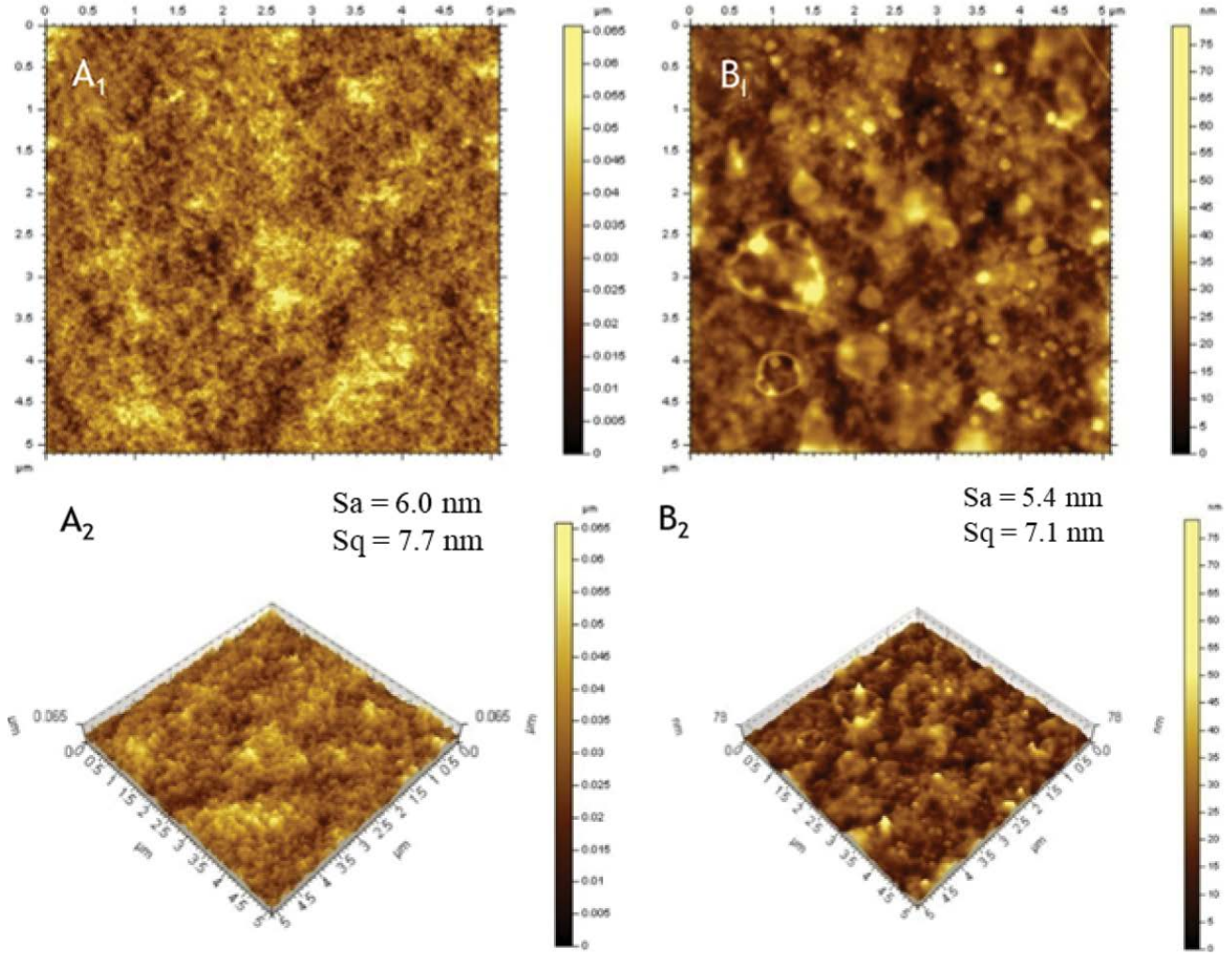

Fig. 9. AFM images of the H-PAN substrate (a) and the PA-TFC membrane (b).

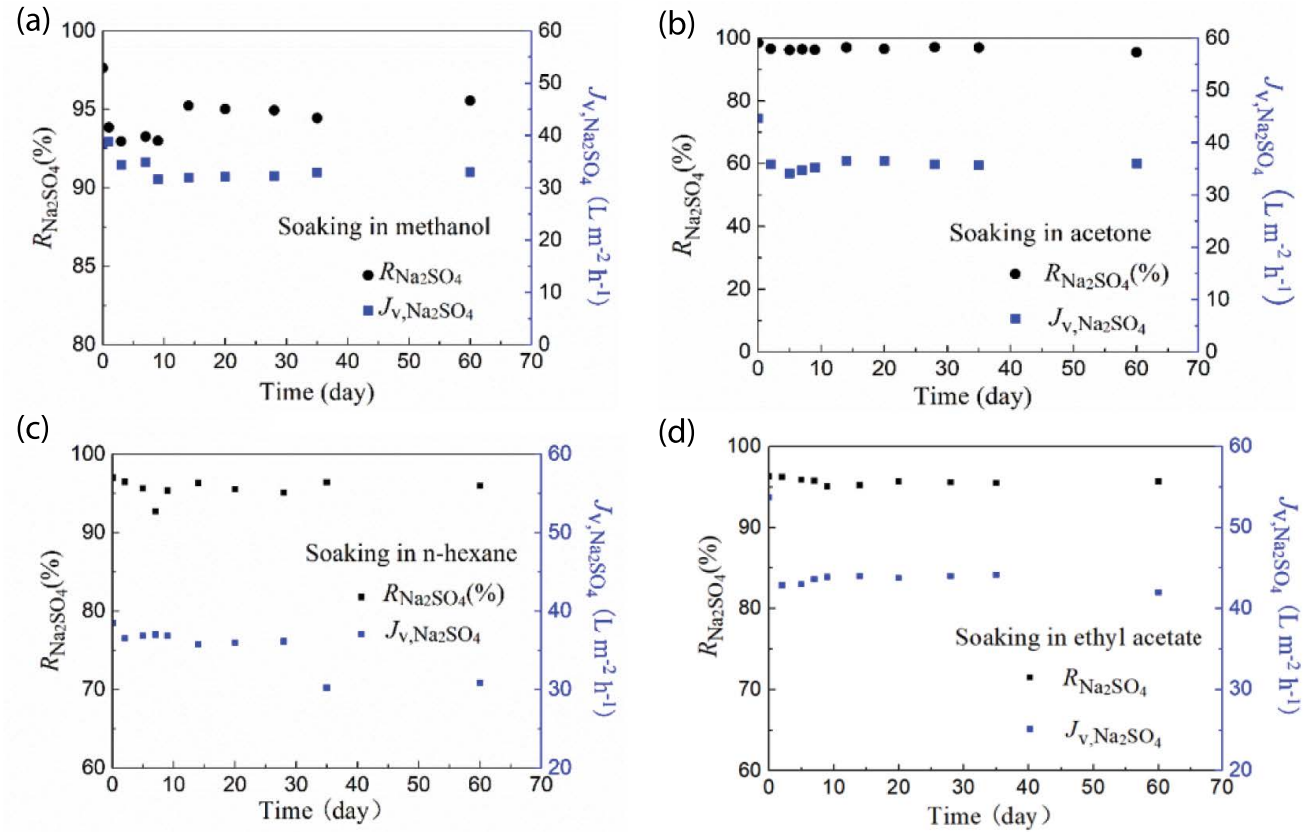

Fig. 11. Separation performance of the prepared PA-TFC membrane after being immersed in (a) methanol, (b) acetone, (c) *n*-hexane and (d) ethyl acetate.

However, after the deposition of PEI, the isoelectric point increased greater than 8.0 owing to the fact that PEI is a positively charged strong polyelectrolyte. After the IP reaction, the isoelectric point decreased down to 5.0. At pH higher than 5.0, the PA composite membrane surface was still negatively charged, which is a strong support of the separation sequence of the inorganic salts shown in Fig. 7.

3.6. Solvent resistance

Fig. 11 depicts the variation of the separation performance of the prepared TFC-PA membrane sheets after being immersed in methanol, acetone, *n*-hexane and ethyl acetate for 60 d, respectively. An apparent decline of both the rejection and the flux was observed at the initial one or several days immersion in polar solvents such as methanol and acetone (Figs. 11a and b). This might be due to the rearrangement of the polymer chains on the membrane surface by the interaction between the membrane polymer and the soaked organic solvent [42,43], as well as the subsequent change of the size and distribution of the pores on the membrane surface [7]. However, for the subsequent nearly 2 months' immersion, the rejection and the flux were relatively stable. The Na_2SO_4 rejection remained higher than 95%, which means that a chemical stable OSN membrane has been successfully fabricated.

For nonpolar solvents, it can be seen from Figs. 11c and d that the rejection and flux also maintained almost stable after immersion in either *n*-hexane or ethyl acetate for 60 d, which indicated that the membrane we fabricated has excellent resistance to the above organic solvents and can be served as OSN membrane.

4. Conclusions

We have prepared a kind of negatively charged polyamide TFC membranes on an alkali-modified PAN ultrafiltration substrate surface via IP reaction using polyethylenimine (PEI) and TMC. The following conclusions can be drawn:

- The addition of NaCl as a kind of supporting electrolyte in the aqueous PEI solution allows conducting of the IP reaction at ultra-low PEI concentration while maintaining a very stable membrane separation performance.
- Optimized membrane preparation conditions were obtained: 0.40 wt.% PEI and 0.50 M NaCl in the aqueous solution; 0.20 wt.% TMC in the organic solution; aqueous immersion of 10 min; IP reaction of 60 s. Under the optimal conditions, the prepared NF membrane could achieve rejections of 97.6% and 66.6%, and fluxes of 38.2 and 43.0 L m^{-2} h^{-1}, for 2,000 mg L^{-1} Na_2SO_4 and NaCl aqueous solutions, respectively, at 1.0 MPa.
- The prepared PA-TFC membranes owned strongly negative charge and showed excellent hydrophilicity at neutral pH. Meanwhile, an ultra-smooth selective layer on the membrane surface was obtained.

- The prepared PA-TFC membranes exhibit excellent resistance to solvents such as methanol, acetone, *n*-hexane, and ethyl acetate. They remained separation performance after being immersed in these solvents for about 60 d.

Acknowledgments

The authors thank the Natural Science Foundation of China (No. 21476218, 20976170) and the Fundamental Research Funds for the Central Universities of China (No. 201822012) for funding support. This is MCTL Contribution No. 179.

References

[1] A.K. Hołda, I.F.J. Vankelecom, Integrally skinned PSf-based SRNF-membranes prepared via phase inversion—Part A: influence of high molecular weight additives, J. Membr. Sci., 450 (2014) 512–521.
[2] Q.C. Xia, J. Wang, X. Wang, B.Z. Chen, J.L. Guo, T.Z. Jia, S.P. Sun, A hydrophilicity gradient control mechanism for fabricating delamination-free dual-layer membranes, J. Membr. Sci., 539 (2017) 392–402.
[3] Q.C. Xia, M.L. Liu, X.L. Cao, Y. Wang, W. Xing, S.P. Sun, Structure design and applications of dual-layer polymeric membranes, J. Membr. Sci., 562 (2018) 85–111.
[4] Z.J. Santanu Karan, Andrew G. Livingston, Sub–10 nm polyamide nanofilms with ultrafast solvent transport for molecular separation, Science, 348 (2015) 1347–1351.
[5] M.F. Jimenez Solomon, Y. Bhole, A.G. Livingston, High flux hydrophobic membranes for organic solvent nanofiltration (OSN) —interfacial polymerization, surface modification and solvent activation, J. Membr. Sci., 434 (2013) 193–203.
[6] M.F. Jimenez Solomon, Y. Bhole, A.G. Livingston, High flux membranes for organic solvent nanofiltration (OSN)—interfacial polymerization with solvent activation, J. Membr. Sci., 423–424 (2012) 371–382.
[7] X.Q. Cheng, K. Konstas, C.M. Doherty, C.D. Wood, X. Mulet, Z. Xie, D. Ng, M.R. Hill, L. Shao, C.H. Lau, Hyper-cross-linked additives that impede aging and enhance permeability in thin polyacetylene films for organic solvent nanofiltration, ACS Appl. Mater. Interfaces, 9 (2017) 14401–14408.
[8] X. Zhang, Y. Lv, H.C. Yang, Y. Du, Z.K. Xu, Polyphenol coating as an interlayer for thin-film composite membranes with enhanced nanofiltration performance, ACS Appl. Mater. Interfaces, 8 (2016) 32512–32519.
[9] W. Fang, L. Shi, R. Wang, Interfacially polymerized composite nanofiltration hollow fiber membranes for low-pressure water softening, J. Membr. Sci., 430 (2013) 129–139.
[10] B. Jiang, H. Zhang, Y. Sun, L. Zhang, L. Xu, L. Hao, H. Yang, Covalent layer-by-layer grafting (LBLG) functionalized super-hydrophobic stainless steel mesh for oil/water separation, Appl. Surf. Sci., 406 (2017) 150–160.
[11] D. Wu, J. Martin, J.R. Du, Y. Zhang, D. Lawless, X. Feng, Effects of chlorine exposure on nanofiltration performance of polyamide membranes, J. Membr. Sci., 487 (2015) 256–270.
[12] D. Wu, Y. Huang, S. Yu, D. Lawless, X. Feng, Thin film composite nanofiltration membranes assembled layer-by-layer via interfacial polymerization from polyethylenimine and trimesoyl chloride, J. Membr. Sci., 472 (2014) 141–153.
[13] X. Bai, Y. Zhang, H. Wang, H. Zhang, J. Liu, Study on the modification of positively charged composite nanofiltration membrane by TiO_2 nanoparticles, Desalination, 313 (2013) 57–65.
[14] H. Zhang, Y. Zhang, L. Li, S. Zhao, H. Ni, S. Cao, J. Wang, Cross-linked polyacrylonitrile/polyethyleneimine–polydimethylsiloxane composite membrane for solvent resistant nanofiltration, Chem. Eng. Sci., 106 (2014) 157–166.
[15] H. Zhang, H. Mao, J. Wang, R. Ding, Z. Du, J. Liu, S. Cao, Mineralization-inspired preparation of composite membranes with polyethyleneimine–nanoparticle hybrid active layer for solvent resistant nanofiltration, J. Membr. Sci., 470 (2014) 70–79.
[16] H. Yang, N. Wang, L. Wang, H.-X. Liu, Q.-F. An, S. Ji, Vacuum-assisted assembly of ZIF-8@GO composite membranes on ceramic tube with enhanced organic solvent nanofiltration performance, J. Membr. Sci., 545 (2018) 158–166.
[17] S.P. Sun, T.A. Hatton, S.Y. Chan, T.-S. Chung, Novel thin-film composite nanofiltration hollow fiber membranes with double repulsion for effective removal of emerging organic matters from water, J. Membr. Sci., 401–402 (2012) 152–162.
[18] C. Ba, D.A. Ladner, J. Economy, Using polyelectrolyte coatings to improve fouling resistance of a positively charged nanofiltration membrane, J. Membr. Sci., 347 (2010) 250–259.
[19] X. Wang, X. Ju, T.Z. Jia, Q.C. Xia, J.L. Guo, C. Wang, Z. Cui, Y. Wang, W. Xing, S.P. Sun, New surface cross-linking method to fabricate positively charged nanofiltration membranes for dye removal, J. Chem. Technol. Biotechnol., 93 (2018) 2281–2291.
[20] G. Hurwitz, G.R. Guillen, E.M.V. Hoek, Probing polyamide membrane surface charge, zeta potential, wettability, and hydrophilicity with contact angle measurements, J. Membr. Sci., 349 (2010) 349–357.
[21] B. Su, T. Wang, Z. Wang, X. Gao, C. Gao, Preparation and performance of dynamic layer-by-layer PDADMAC/PSS nanofiltration membrane, J. Membr. Sci., 423–424 (2012) 324–331.
[22] S. Yang, H. Zhen, B. Su, Polyimide thin film composite (TFC) membranes via interfacial polymerization on hydrolyzed polyacrylonitrile support for solvent resistant nanofiltration, RSC Adv., 7 (2017) 42800–42810.
[23] G. Zhang, H. Yan, S. Ji, Z. Liu, Self-assembly of polyelectrolyte multilayer pervaporation membranes by a dynamic layer-by-layer technique on a hydrolyzed polyacrylonitrile ultrafiltration membrane, J. Membr. Sci., 292 (2007) 1–8.
[24] T. Ma, Y. Su, Y. Li, R. Zhang, Y. Liu, M. He, Y. Li, N. Dong, H. Wu, Z. Jiang, Fabrication of electro-neutral nanofiltration membranes at neutral pH with antifouling surface via interfacial polymerization from a novel zwitterionic amine monomer, J. Membr. Sci., 503 (2016) 101–109.
[25] N. Wang, S. Ji, G. Zhang, J. Li, L. Wang, Self-assembly of graphene oxide and polyelectrolyte complex nanohybrid membranes for nanofiltration and pervaporation, Chem. Eng. J., 213 (2012) 318–329.
[26] W. Shan, P. Bacchin, P. Aimar, M.L. Bruening, V.V. Tarabara, Polyelectrolyte multilayer films as backflushable nanofiltration membranes with tunable hydrophilicity and surface charge, J. Membr. Sci., 349 (2010) 268–278.
[27] R.A. McAloney, M. Sinyor, V. Dudnik, M.C. Goh, Atomic force microscopy studies of salt effects on polyelectrolyte multilayer film morphology, Langmuir, 17 (2001) 6655–6663.
[28] K. Büscher, K. Graf, H. Ahrens, C.A. Helm, Influence of adsorption conditions on the structure of polyelectrolyte multilayers, Langmuir, 18 (2002) 3585–3591.
[29] Y. Cui, H. Wang, H. Wang, T.-S. Chung, Micro-morphology and formation of layer-by-layer membranes and their performance in osmotically driven processes, Chem. Eng. Sci., 101 (2013) 13–26.
[30] R. Malaisamy, M.L. Bruening, High-flux nanofiltration membranes prepared by adsorption of multilayer polyelectrolyte membranes on polymeric supports, Langmuir, 21 (2005) 10587–10592.
[31] S.U. Hong, M.L. Bruening, Development of polyion complex membranes based on cellulose acetate modified by oxygen plasma treatment for pervaporation, J. Membr. Sci., 280 (2006) 1–5.
[32] S.U. Hong, R. Malaisamy, M.L. Bruening, Optimization of flux and selectivity in Cl^-/SO_4^{2-} separations with multilayer polyelectrolyte membranes, J. Membr. Sci., 283 (2006) 366–372.
[33] P. Wen, Y. Chen, X. Hu, B. Cheng, D. Liu, Y. Zhang, S. Nair, Polyamide thin film composite nanofiltration membrane modified with acyl chlorided graphene oxide, J. Membr. Sci., 535 (2017) 208–220.
[34] X.-l. Wang, J.-f. Wei, Z. Dai, K.-y. Zhao, H. Zhang, Preparation and characterization of negatively charged hollow fiber nanofiltration membrane by plasma-induced graft polymerization, Desalination, 286 (2012) 138–144.
[35] F.-Y. Zhao, Q.-F. An, Y.-L. Ji, C.-J. Gao, A novel type of polyelectrolyte complex/MWCNT hybrid nanofiltration

membranes for water softening, J. Membr. Sci., 492 (2015) 412–421.
[36] X. Wang, H. Wang, Y. Wang, J. Gao, J. Liu, Y. Zhang, Hydrotalcite/graphene oxide hybrid nanosheets functionalized nanofiltration membrane for desalination, Desalination, 451 (2019) 209–218.
[37] F.Y. Zhao, Y.L. Ji, X.D. Weng, Y.F. Mi, C.C. Ye, Q.F. An, C.J. Gao, High-flux positively charged nanocomposite nanofiltration membranes filled with poly(dopamine) modified multiwall carbon nanotubes, ACS Appl. Mater. Interfaces, 8 (2016) 6693–6700.
[38] J. Gao, S.-P. Sun, W.-P. Zhu, T.-S. Chung, Green modification of outer selective P84 nanofiltration (NF) hollow fiber membranes for cadmium removal, J. Membr. Sci., 499 (2016) 361–369.
[39] L.D. Nghiem, S. Hawkes, Effects of membrane fouling on the nanofiltration of pharmaceutically active compounds (PhACs): mechanisms and role of membrane pore size, Sep. Purif. Technol., 57 (2007) 176–184.
[40] A. Bera, J.S. Trivedi, S.K. Jewrajka, P.K. Ghosh, In situ manipulation of properties and performance of polyethyleneimine nanofiltration membranes by polyethylenimine-dextran conjugate, J. Membr. Sci., 519 (2016) 64–76.
[41] S. Zhao, Z. Wang, A loose nano-filtration membrane prepared by coating HPAN UF membrane with modified PEI for dye reuse and desalination, J. Membr. Sci., 524 (2017) 214–224.
[42] B. Van der Bruggen, J. Geens, C. Vandecasteele, Fluxes and rejections for nanofiltration with solvent stable polymeric membranes in water, ethanol and *n*-hexane, Chem. Eng. Sci., 57 (2002) 2511–2518.
[43] B. Van der Bruggen, J. Geens, C. Vandecasteele, Influence of organic solvents on the performance of polymeric nanofiltration membranes, Sep. Sci. Technol., 37 (2002) 783–797.